In Situ Fiber-Reinforced Composites from Blends Containing Polypropylene and Polycaprolactone

Takeshi Semba,[1] Kazuo Kitagawa,[1] Satoshi Endo,[2] Kazunori Maeda,[2] Hiroyuki Hamada[3]

[1]*Department of Applied Chemistry, Kyoto Municipal Institute for Industrial Research, 17 Chudoji Minami-machi, Shimogyo-ku, Kyoto 600-8813, Japan*
[2]*Technology and Development Department, Hexa Chemical Company, Ltd., 153 Yokomakura-Nishi, Higashi-Osaka-City 578-0956, Japan*
[3]*Division of Advanced Fibro-science, Kyoto Institute of Technology, Goshokaido-cho, Matsugasaki, Sakyo-ku, Kyoto 606-8585, Japan*

Received 24 June 2002; accepted 25 April 2003

ABSTRACT: Our study was focused on the presupposition that morphology control in immiscible polymer blend could give rise to reinforcement in composites. To investigate the effects of shear and elongational flow in polymer processing, observation of the mechanical properties and the morphology of the polypropylene/polycaprolactone (PP/PCL) blend system was performed. PP/PCL sheets were fabricated by means of a single-screw extruder equipped with a slit-type die to which high shear and elongational stresses were applied. For the sake of comparison, a second series of composites of identical composition was compression molded with a hot-press machine that transmits lower shear and elongational stresses. The results indicate that the extruded sheets have better mechanical properties than those of the compression-molded sheets, a result attributed to the generation of *in situ* dispersed long fiber minor phases and cocontinuous phases in the extruded composites. The differences in the crystallization behavior of the fibrous and spherically shaped components were indicated clearly by DSC curves. A PP crystalline peak indicative of *in situ* PP fiber formation is conspicuous around 980 cm^{-1} (PP crystalline band) in the FTIR spectrum. © 2003 Wiley Periodicals, Inc. J Appl Polym Sci 91: 833–840, 2004

Key words: blends; shear; immiscibility; stress; morphology

INTRODUCTION

One of the major topics in polymer blends is morphology control of dispersed components that can show a high or functional performances. Several studies concerning this control have been carried out and applied in industrial products.[1]

Takayanagi[2,3] proposed the concept of "molecular composites," in which the dispersed size of liquid crystalline polymer (LCP) components achieve nanodimension in the matrix. The LCPs have excellent mechanical, heat resistance, and good processing properties. Furthermore, the LCP component formed spherical and fibril reinforcements in these systems, and it was clear that the dispersed phase played an important role in the mechanical properties of molecular composites.[4–10] In the LCP blend systems, the blend ratio, the viscosity ratio, the interface between LCP and a matrix resin, and other processing conditions considerably influenced both the morphology and the size of the dispersed phase. The size of the LCP dispersed phase is from 0.1 to 100 μm.

Correspondence to: T. Semba (sentake@city.kyoto.jp).

Journal of Applied Polymer Science, Vol. 91, 833–840 (2004)

Fakirov et al.[11–15] investigated microfibril composites of a poly(ethylene teraphthalate)/poly(amide-6) (PET/PA6) blend system. In their SEM observations and X-ray diffraction measurement, the PET component formed the microfibril that oriented along the flow direction. The microfibril, however, was not sufficient reinforcement for the composites because of their mechanical properties.

Kitagawa et al.[16] found peculiar morphology in low-density polyethylene/poly(butylene/terephthalate (LDPE/PBT)) blend systems such that the PBT dispersive phase was a continuous long fiber rather than a fibril. The generation of *in situ* long continuous fibers of PBT in the LDPE matrix was observed. The drawing on extrusion affected the mechanical properties and morphology of the extrudate strands. In the injection molding of pellets obtained from the drawn strands, the most suitable processing temperature was used, which was slightly below the PBT melting point. The injection moldings possessed the *in situ* PBT reinforcement in the LDPE matrix. Furthermore, a LDPE/polycaprolactone (PCL) blend system in which the melting point of PCL is lower than that of LDPE also showed that *in situ* LDPE long-fiber reinforcement occurred in the PCL matrix.[17] The tensile moduli of these blends exceeded the theoretical line calculated

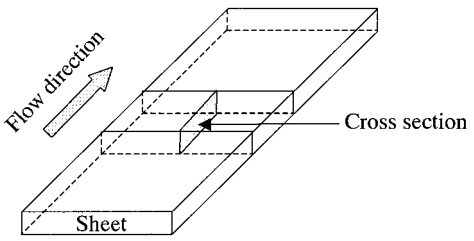

Figure 1 Schematic diagram of the cross section for FTIR analysis.

by the rule of mixtures, but were not satisfactory composites.

Michel et al.[18–21] reported the solvent permeability and drawing conditions of the high-density polyethylene/(HDPE)/PBT blend system. PBT fibrillar morphology was made for antisolvent permeability attributed to the tortuous path of hydrocarbon molecules. Recently they introduced the "dynamic quenching process" for ethylene vinyl acetate (EVA)/PBT [or bisphenol-A polycarbonate (PC)] blend systems.[22] In this process, the barrel temperature was gradually increased toward the upstream of the extruder. Interesting morphologies such as coral-shaped PBT and rod-shaped PC formed in the EVA matrix, arising from the effective prevention of breakup and coalescence during processing.

Except for the LCP system, most microfibril composites in polymer blends do not have adequate mechanical properties. However, from several years of research, the authors found that the mechanical properties of *in situ* fiber-reinforced polypropylene (PP)/PCL blend showed multiple effects without a compatibilizer.[23] At present, PCL is well known as a biodegradable polymer, but the first use of PCL was as an additive for improving the properties of plastic materials, for example, improvements of impact strength and so on.

Our study has been focused on the presupposition that morphology control in an immiscible polymer blend system could give rise to reinforcement in composites. We have designated them *in situ* fiber-reinforced composites. The aim of this study was to investigate the effects of shear and elongational flow in polymer processing on the mechanical properties and the morphology of the PP/PCL blend system.

EXPERIMENTAL

Materials

The materials used in this study were a PP (Idemitsu PP J900GP, MI = 13, M_W = 200,000; Idemitsu Petrochemical Co., Ltd.) and a PCL (Celgreen PH7, MI = 2.4; Daicel Chemical Industries, Ltd).

Fabrication of PP/PCL blend sheets

Compression molding

Compression molding, a processing method with low shear and elongational flow, was used to fabricate the PP/PCL blend sheets. First, the 3PP and PCL pellets were gradually added to a batch-type mixer (Labo Plastomill 100C100; Toyoseikiseisaku-sho Ltd.) at 200°C and a screw revolution of 30 rpm for 90 s. The compositions of the PP/PCL blend were 0/10, 2/8, 5/5, 8/2, and 10/0 by weight.

The compounds were held between two aluminum plates, with polished Teflon surfaces, and compression molded with a heat press machine (NF-50; max load = 50 tf Shinto Metal Industries Ltd.). Compression-molding conditions were as follows: compressive pressure, 0.3 MPa; processing time, 60 s. The resulting sheets were quenched immediately in water. The thickness of the sheets was about 1 mm.

Extrusion

PP/PCL blend sheets were fabricated using a single-screw extruder with a screw length to diameter ratio

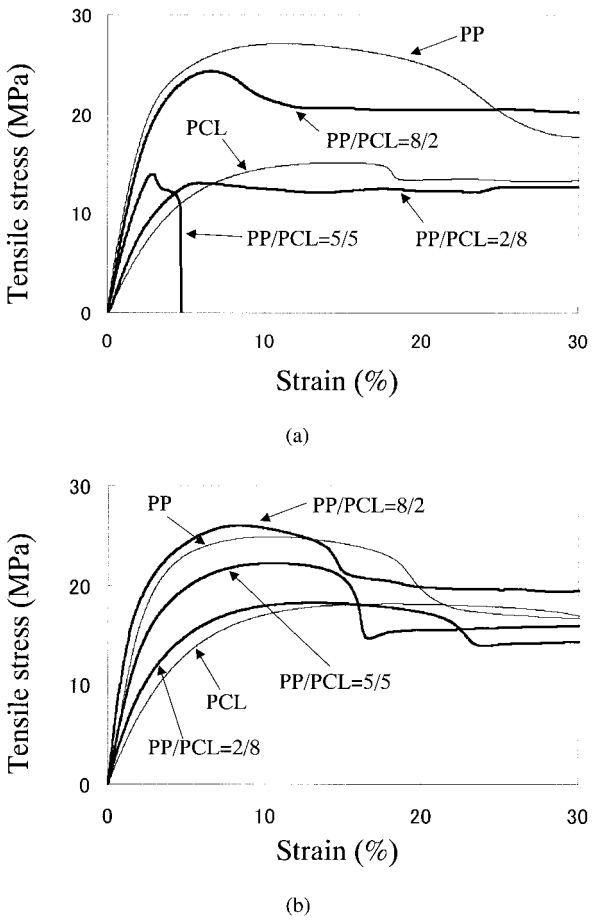

Figure 2 Typical tensile stress–strain curves of (a) compression-molded PP/PCL blended sheets, (b) extruded PP/PCL blended sheets.

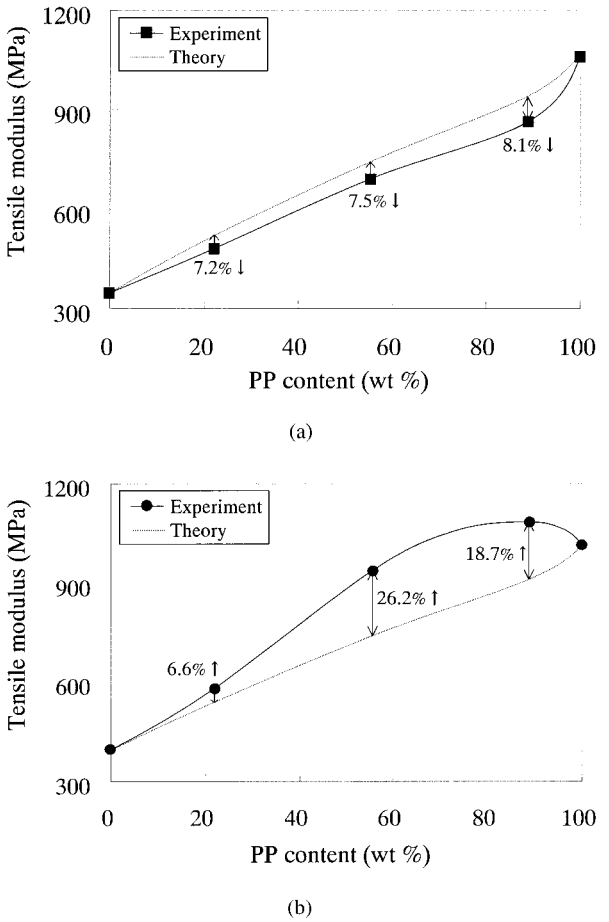

Figure 3 Relationship between PP content and tensile modulus of (a) compression-molded PP/PCL blended sheets, (b) extruded PP/PCL blended sheets.

(L/D) of 32 (PSV30 : Pula Enge Co., LTD.) equipped with slit type die (t = 1 mm), and a drawing machine. This setup generated high shear flow and high elongational flow. The barrel temperature used was between 170 and 200°C ranging from the hopper to the die. The screw revolution was fixed to maintain the thickness of the sheets at 1 mm. The drawing rate was 715 cm/min and the extruded sheet was water cooled. The compounding ratios of the PP/PCL blends were identical to those of compression molding.

Mechanical properties

Tensile testing of the blended sheets along the flow direction was performed with a universal testing machine (Autograph AG-5000E; Shimadzu, Kyoto, Japan) at a crosshead speed of 5 mm/min and at room temperature. The tensile gauge length was 50 and 65 mm for the compression-molded and extruded sheets, respectively.

Morphology

To facilitate an effective SEM observation, the PCL component of the blend sheets was extracted using chloroform by a Soxhlet extractor. The surfaces of the residual PP were observed by SEM (JSM 5900-LV; JEOL Ltd., Tokyo, Japan). The skin area where the depth from surface is 100 μm and the core area were observed in the extrudates.

FTIR and DSC analysis

Attenuated total reflectance (ATR) spectra in the 4000–600 cm^{-1} region were measured by use of an FTIR spectrometer (System 2000 FTIR (Perkin Elmer Cetus Instruments, Norwalk, CT)); detector: TGS; resolution: 4 cm^{-1}] on the cross section, shown in Figure 1, along the flow direction. The analytical specimens were obtained by breaking the sheet after immersion in liquid nitrogen. ATR measurements were carried out by putting the cross section directly on the diamond internal reflectance element (IRE), a 2-mm square window.

Thermal analysis of the same specimens used above for FTIR analysis was carried out by differential scanning calorimetry (DSC 7; Perkin–Elmer heating rate: 10°C/min).

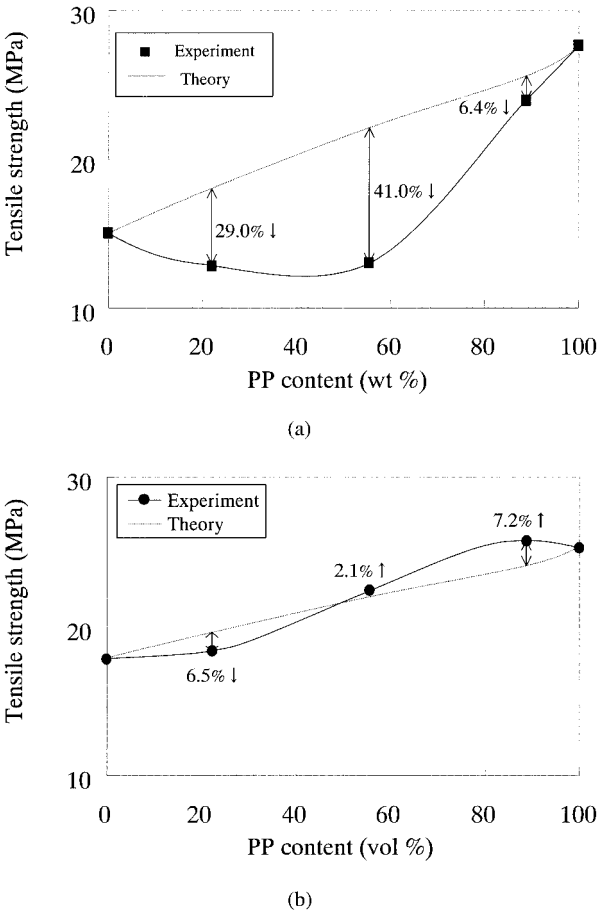

Figure 4 Relationship between PP content and tensile strength of (a) compression-molded PP/PCL blended sheets, (b) extruded PP/PCL blended sheets.

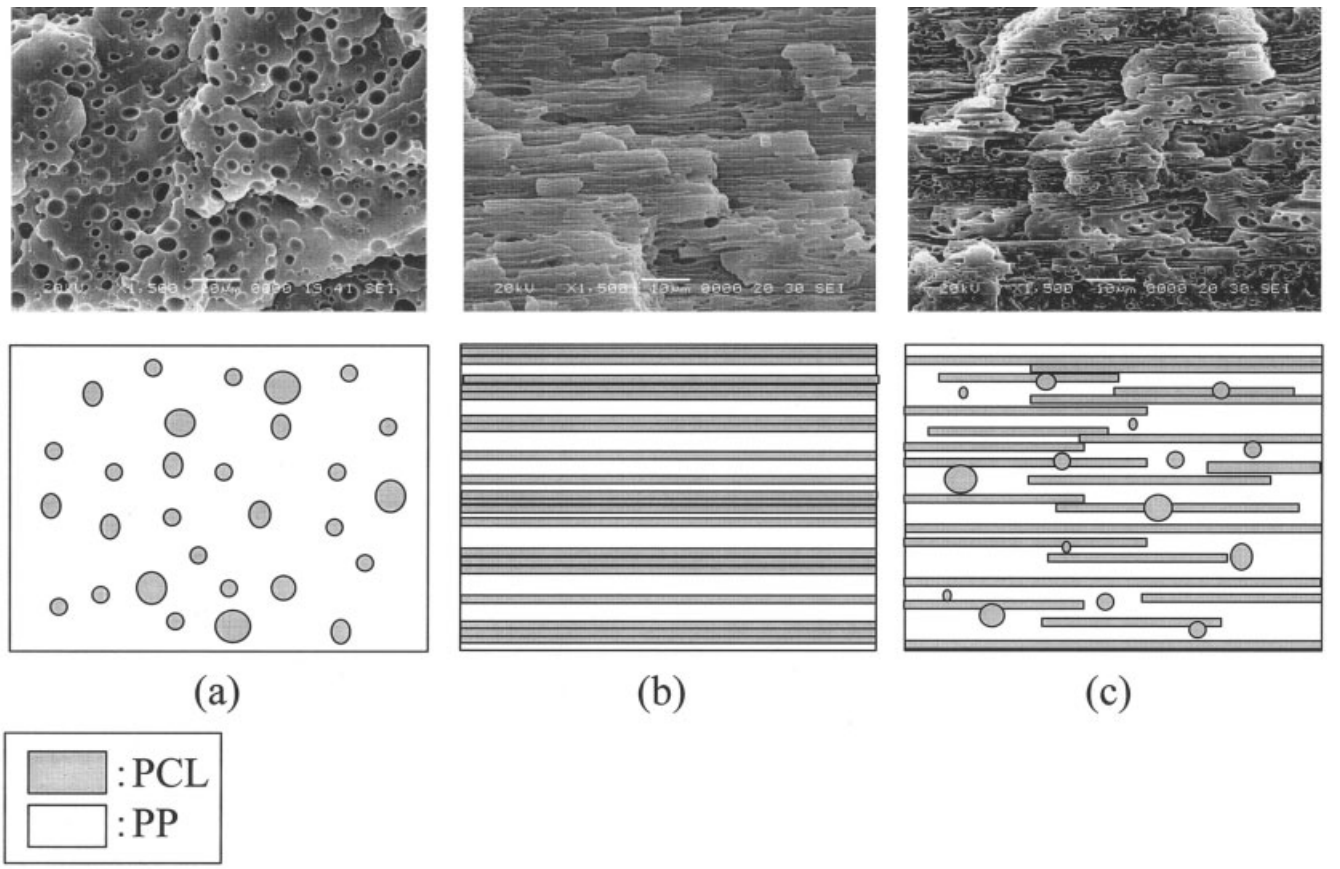

Figure 5 Scanning electron micrographs and schematic diagrams of the PP/PCL = 8/2 sheets: (a) compression-molded sheet; (b) skin layer in extruded sheet; (c) core layer in extruded sheet.

RESULTS AND DISCUSSION

Tensile properties

Typical stress–strain curves obtained from the compression-molded samples are shown in Figure 2(a), whereas those from extruded sheets are shown in Figure 2(b). In Figure 2(a), the 5/5 PP/PCL blend has undergone brittle fracture at 4.1% strain. On the contrary, the 5/5 blend in Figure 2(b) displayed ductile behavior with a prominent yield peak before necking and cold drawing with an ultimate nominal strain above 50%. This is an indication of reinforcement, given that the two components behaved cohesively and displayed a behavior similar to that of the net resins (i.e., PP and PCL).

Figure 3(a) and (b) show the relationship between PP content and tensile modulus of the blended sheets for both processing methods. The tensile moduli of the compression-molded sheets fall below the theoretical line [Fig. 3(a)]. On the other hand, the values from the extruded sheets were considerably higher than the theoretical line at all compositions (rule of mixtures). The increase of moduli above the theoretical line of extruded sheets was 6.6, 26.2, and 18.7% for the 2/8, 5/5, and 8/2 sheets, respectively. Furthermore, the tensile modulus of the 8/2 blended sheets exceeded that of the neat PP sheets by 6.7% [Fig. 3(b)]. This synergism in tensile modulus is an indication that the extrusion is an effective processing method for these composites.

Figure 4(a) and (b) show the relationship between tensile strength and PP content for both types of blends. The tensile strengths of the compression-molded sheets showed the typical tendency of immiscible polymer blends; thus the values were undoubtedly below the theoretical line. In Figure 4(a), the tensile strengths of the compression-molded 2/8 PP/PCL blend showed a value that almost remained constant to 5/5 compositions, and then increased from 5/5 to 10/0 compositions. However, the tensile strength of the extruded sheets exhibited excellent tensile strength. The values were in some cases higher than the theoretical line values: −6.5, 2.1, and 7.2% for the 2/8, 5/5, and 8/2 PP/PCL blends, respectively [Fig. 4(b)]. The above results confirmed that the shear and elongational flow in the extrusion process modified the tensile properties of the extrudates. It could therefore be inferred that the contrast in tensile strength resulted from the differences in the internal

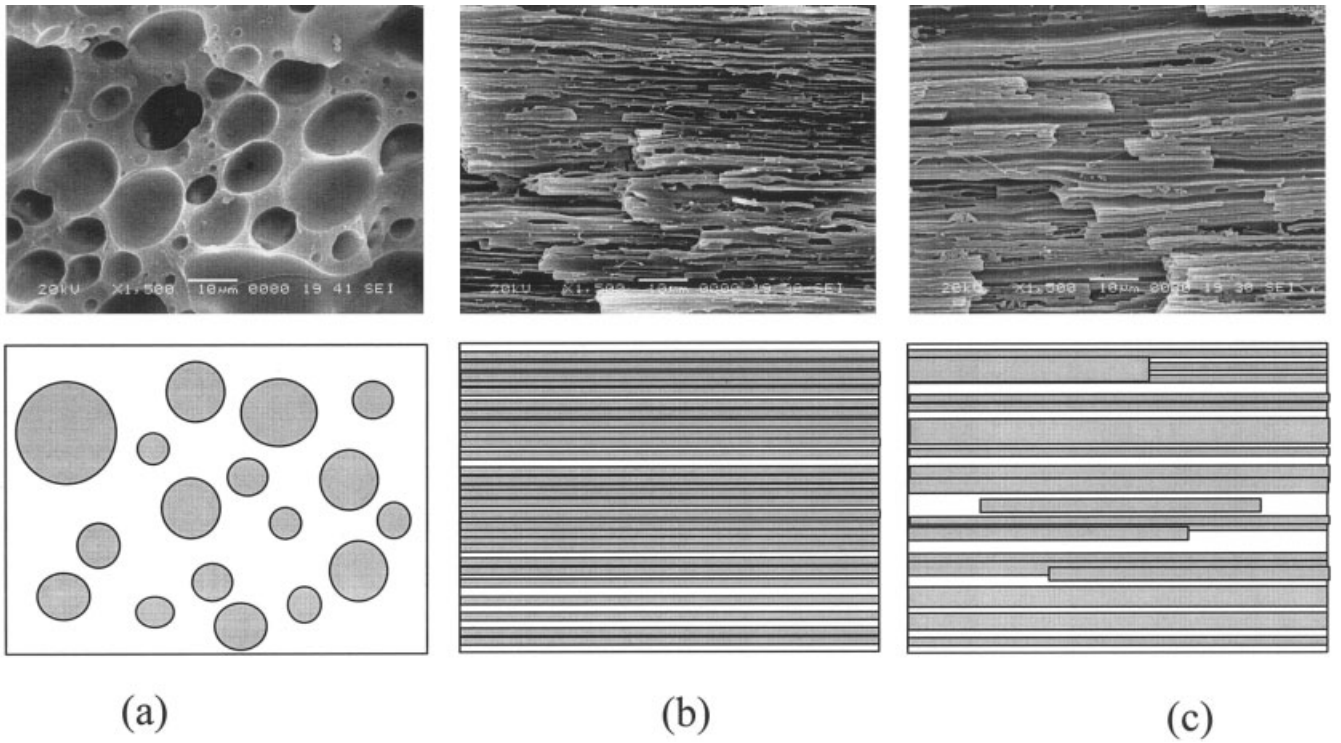

Figure 6 Scanning electron micrographs and schematic diagrams of the PP/PCL = 5/5 sheets: (a) compression-molded sheet; (b) skin layer in extruded sheet; (c) core layer in extruded sheet.

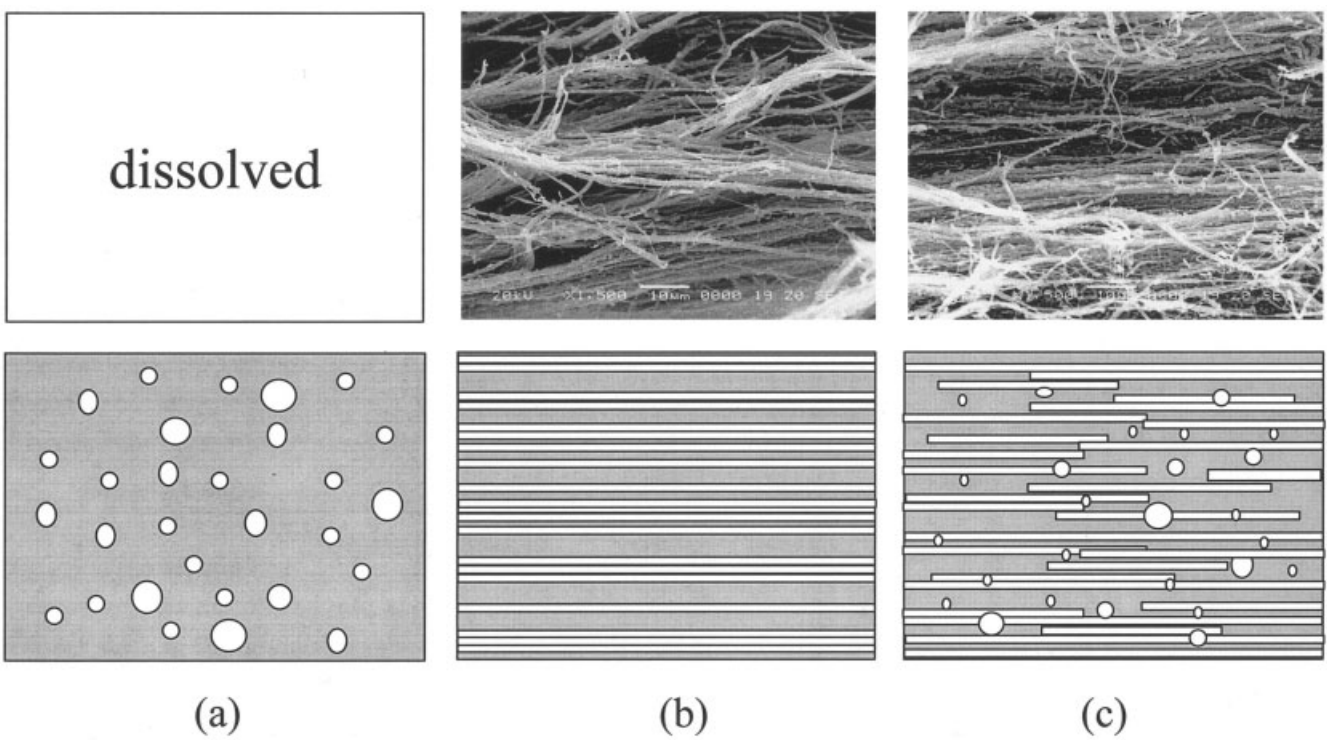

Figure 7 Scanning electron micrographs and expected schematic diagrams of the PP/PCL = 2/8 sheets: (a) compression-molded sheet; (b) skin layer in extruded sheet; (c) core layer in extruded sheet.

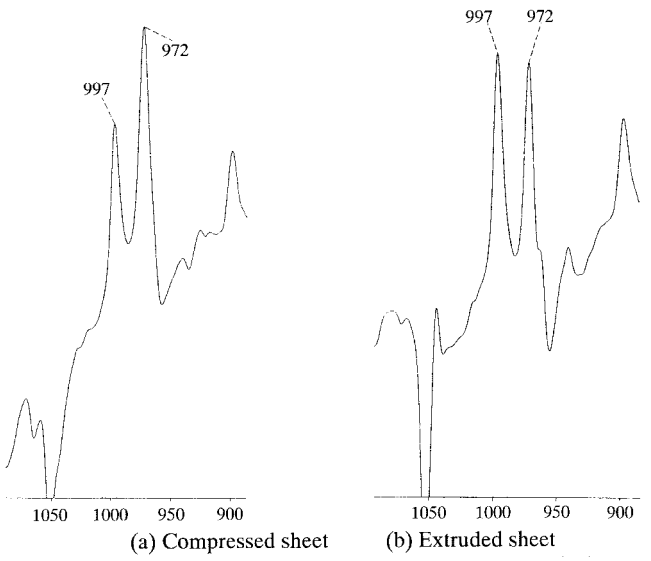

Figure 8 Difference FTIR spectra for the PP/PCL = 2/8 sheets obtained after subtracting the spectrum of neat PCL.

structures of the blends, which are consequences of the processing methods used.

Morphology

Figure 5 shows the scanning electron micrographs (SEM) of the 8/2 PP/PCL blends fabricated by both methods. The PCL component of the compression-molded sheets was extracted with chloroform so the black spherical cavities indicate PCL [Fig. 5(a)]. The sizes of the cavities range from 0.3 to 8 μm. The schematic diagram illustrates the distribution of PCL droplets in the PP phase. In the case of the extruded sheets, the PCL components at the skin layer exposed to shear flow formed long fibers along the flow direction. The number of the droplets gradually increased in the core layer, attributed to the low shear flow and the relaxation of orientation resulting from the quenching rate difference between the surface and the core [Fig. 5(b), (c)].

SEM micrographs of 5/5 PP/PCL for both blends are shown in Figure 6. In the compression-molded sheets, the PCL domains of spherical shape with various sizes are dispersed in the PP matrix [Fig. 6(a)]. The droplet sizes are much larger than those of the 8/2 blend as a result of domain coalescence [Fig. 6(a)]. The morphology of the extruded sheets is a cocontinuous structure in both skin and core layers [Fig. 6(b), (c)].

Figure 7 shows the morphology of the 2/8 PP/PCL blend sheets. The PCL matrix was dissolved by chloroform, so that the PP dispersed phase can be seen in these micrographs. The compression-molded sheets were completely dissolved by the chloroform. Therefore, it is assumed that the PP component in these sheets must be distributed with a very fine spherical shape. The expected morphology is shown in the schematic diagram [Fig. 7(a)]. Fine continuous fiber and net shape reinforcements were clearly dispersed from the skin to the core layer in the extruded sheet, as shown in Figure 7(b) and (c). Based on these results, it could be inferred that the minor component in the PP/PCL blend sheets is deformed into continuous long fibers as a consequence of shear and elongational flow; the long fibers thus effectively reinforced the matrix.

The mechanism of fiber formation in this process may be elucidated as follows: the dispersed components are initially fixed as droplets by the screw compounder and the shear flow in the slit-type die transforms these droplets into long fibers. Furthermore, the elongational flow between the die lip and the quenching zone accelerates fiber formation.

The well-known equation expressed for droplet deformation is capillary number:

$$\mathrm{Ca} = \tau/(\sigma/R)$$

where τ is shear or elongational stress, σ is interfacial tension, and R is droplet radius. Ca_{crit} is defined as the breakup of a droplet. An index $\mathrm{Ca}/\mathrm{Ca}_{crit}$ corresponds to deformation type of droplet such as nondeformation, breakup, and deformation into fiber. The dispersed droplet can deform into fiber shape only when the $\mathrm{Ca}/\mathrm{Ca}_{crit}$ is greater than 4.[25–27]

The authors studied some combinations of *in situ* fiber-reinforced composites and found that all of them are mixtures of low and high surface tension materials. It is therefore expected that the interfacial tension is large. The values of surface tension of PP and PCL

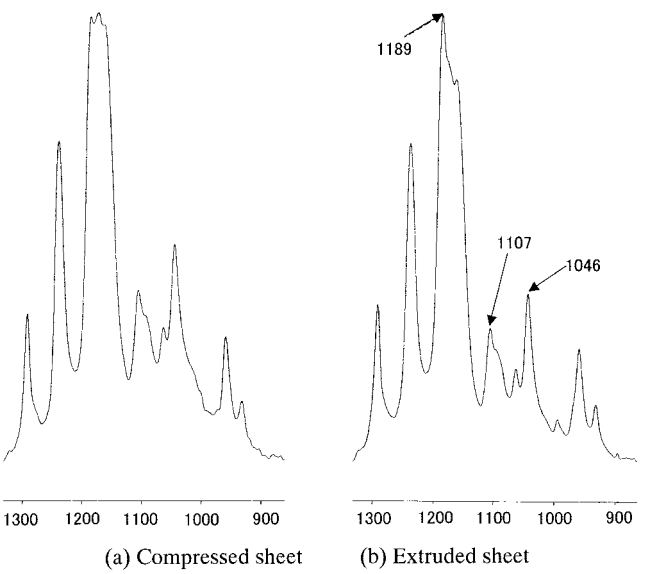

Figure 9 Difference FTIR spectra for the PP/PCL = 8/2 sheets obtained after subtracting the spectrum of neat PP.

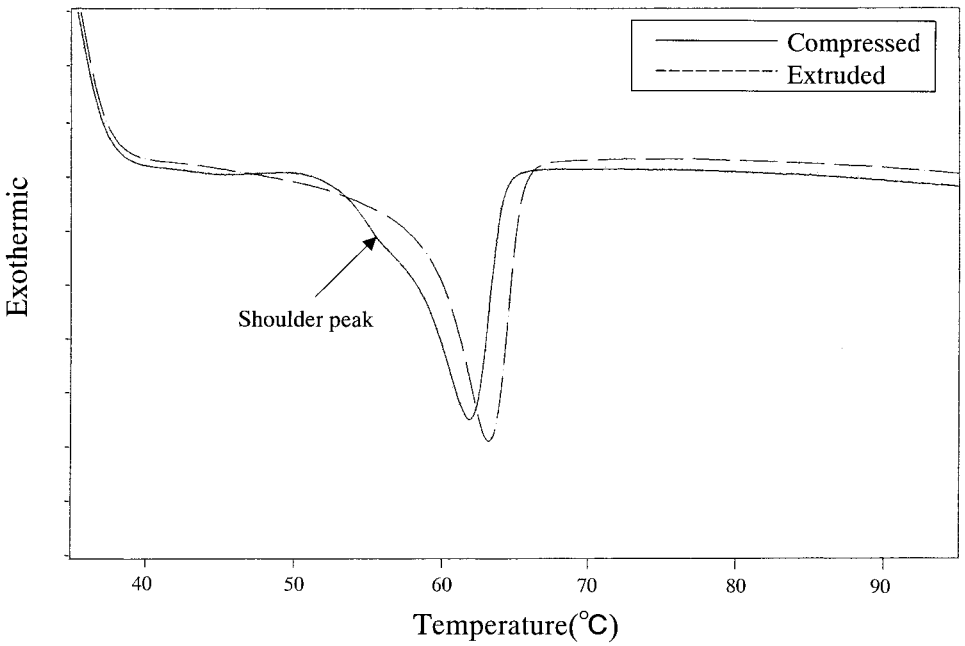

Figure 10 DSC thermograms of the compression molded and extruded sheets for the PP/PCL = 8/2 composition.

are 20.7 and 35.3 mN/m, respectively, at 200°C, as determined by the pendant drop method. Based on these figures, it can be seen that the interfacial tension of the PP/PCL system is substantial. Mason[28] observed four distinct deformation modes of behavior. In one of these deformation modes, the drop extended into a long thread when the interfacial tension is large.

Evaluation of crystallinity

Figure 8 shows the difference FTIR spectra obtained by subtracting the spectrum of neat PCL from the spectra of the compression-molded and extruded sheets, respectively, for the 2/8 PP/PCL composition. The resulting spectra represent the spectra of the PP component arising from both blending processes. The characteristic band at 997 cm^{-1} is called the crystalline band of PP. The 997/972 cm^{-1} ratio is usually evaluated as the crystallinity of PP.[29] The 997/972 cm^{-1} value for the spectrum of the extruded 2/8 PP/PCL sheet was 1.04. Nevertheless, that of the compression-molded 2/8 PP/PCL sheet was 0.78. It became obvious that the PP fiber component in the extruded 2/8 PP/PCL sheets had higher crystallinity than that in the compression-molded sheets.

Similarly, Figure 9 shows the difference spectra of the neat PP sheets from both processed sheets of the 8/2 PP/PCL blend. These spectra indicated the spectrum of PCL component arising from both blending methods. It can be seen that the shape of the absorption band around 1170 cm^{-1}, based on C—O stretching vibration of the PCL, is quite different depending on the processing method. Furthermore, the band heights of the 1107 and 1046 cm^{-1} bands of the extruded sheet are smaller compared to those of the compressed sheet. These tendencies were discovered by the authors in a previous study, which revealed that morphology differences exists between the two types of dispersed phases.[23] Because PCL is a crystalline resin, it is expected that the crystallinity will be different depending on the dispersed morphology that arises from the processing method.

The DSC thermograms of the 8/2 PP/PCL sheets manufactured by both methods are shown in Figure

TABLE I
Melting Enthalpy of the Blend Sheets[a]

	PCL		8/2		5/5		2/8		PP	
	PCL	PP	PCL	PP	PCL	PP	PCL	PP	PCL	PP
(a) Press	71.30	×	70.81	74.33	71.58	78.69	62.14	81.04	×	78.15
(b) Extrusion	76.40	×	71.35	81.30	74.95	79.39	75.21	78.44	×	78.75
(b) − (a)	5.10	×	0.54	6.97	3.37	0.70	13.07	−2.60	×	0.60

[a] Units in J/g^{-1}.

10. The thermograms of the two processes differ around 60°C depending on the processing method. The compression-molded sheet has a shoulder peak at 55.6°C aside from the main peak, indicating the existence of a microcrystal structure. The crystal of extruded sheets is characteristically homogeneous so the peak shape is smooth.

Table I summarizes the melting enthalpy data (ΔH) from DSC analysis. In the case of 8/2 PP/PCL the ΔH_{PCL} values of the compressed and the extruded sheets were 75.21 and 62.14 J/g, respectively. The deformation from the droplet to fiber shape of the PCL dispersed phase in the extrudate exerts substantial influence on ΔH_{PCL}. On the other hand, the shape of the PP endothermic part and the ΔH_{PP} are almost the same, indicating that the crystal structure and the crystallinity of the matrix are not affected by shear and elongational flow in the extruder. In the case of 5/5 PP/PCL, the shoulder peak of the PCL endothermic part was observed in both processes. This phenomenon of only a slight increase of the ΔH_{PCL} and ΔH_{PP} indicates that the dispersed phase formed a cocontinuous structure, as shown in Figure 6(b) and (c).

The PP fiber reinforcements were shaped in the extruded 2/8 PP/PCL sheets in which the matrix is the PCL. The ΔH_{PP} value of the fiber reinforcements in the extruded sheets was also higher than that of the compressed sheet. This is in accordance with the results based on FTIR analysis as discussed earlier. Some previous studies, for instance, proved that crystallinity of isotactic polypropylene under shear flow increased as nucleation was induced by shear flow.[30, 31] In the PP/PCL blend system, the high crystallinity of the fibrous dispersed phase originated from shear and elongational flow efficiently conveying the dispersed phase through the interface (between matrix and dispersion) by special matching of PP and PCL. FTIR and DSC analysis revealed that the crystallinity of the fiber reinforcement is induced by shear and elongational flow.

CONCLUSIONS

The effects of shear and elongational flow in polymer processing on mechanical properties and the morphology of the PP/PCL blend system, which was one of the *in situ* fiber-reinforced composites, were investigated.

1. The combined effect of shear and elongational flows in processing prompted the dispersed phase to transform into long-fiber reinforcements.
2. The synergism in tensile strength and tensile modulus is a very strong indication that *in situ* fiber formation caused reinforcement.
3. The component with low blend ratio formed the continuous long-fiber reinforcements in the matrix, which were composed of individual fibers or net fibers. On the other hand, the equivalent blend as the 5/5 PP/PCL had a cocontinuous structure resembling multilayers.
4. The peculiar peak in the FTIR spectrums appeared in the extruded sheets, whereas the enthalpy of the fibrous components increased in contrast to the spherical dispersions. The results obtained from these analyses indicated that higher crystallinity was achieved in the fibrous components.

References

1. Utracki, L. A. Polymer Alloys and Blends; Hanser: New York, 1989.
2. Takayanagi, M. Polym Prepr Jpn 1987, 36, 3060.
3. Takayanagi, M. In: Preprints of IUPAC 32nd International Symposium on Macromolecules, Preprint 36, 1988.
4. Crevecoeur, G.; Groeninckx, G. Polym Eng Sci 1990, 30, 532.
5. Isayev, A.; Modic, M. Polym Compos 1987, 8, 158.
6. Weiss, R. A.; Huh, W.; Nicolais, L. Polym Eng Sci 1987, 27, 684.
7. Subramanian, P. R.; Isayev, A. I. SPE Tech Pap 1990, 48, 489.
8. Weiss, R. A.; Chung, N. S.; Dutta, D. ACS Prepr 1987, 30, 544.
9. (a) Kiss, G. Polym Eng Sci 1987, 27, 410; (b) Macromolecular Systems; Culbertson, B. M., Ed.; Plenum Press: New York, 1989.
10. Shibata, M.; Zhu, X.; Yosomiya, R. Polym Polym Compos 1998, 6, 433.
11. Evastatiev, M.; Nicolov, N.; Fakirov, S. Polymer 1996, 37, 4455.
12. Kardos, J. L.; Fakirov, S. J Polym Sci Eng 1995, 15, 183.
13. Fakirov, S.; Evastatiev, M.; Schultz, J. M. Polymer 1993, 34, 4669.
14. Evastatiev, M.; Schultz, J. M.; Fakirov, S.; Friedrich, K. Polym Eng Sci 2001, 41, 192.
15. Fakirov, S.; Stribeck, N. J Macromol Sci Phys 2001, 40, 935.
16. Kitagawa, K.; Semba, T.; Hamada, H. J Mater Sci Jpn 1998, 47, 1270.
17. Semba, T.; Kitagawa, K.; Hamada, H. In: Proceedings of the 6th Japan International SAMPE Symposium, October 26–29, 1999; p. 921.
18. Cassagnau, P.; Fulchiron, R.; Michel, A. J Polym Sci Part B: Polym Phys 1998, 36, 2573.
19. Monticciolo, A.; Cassagnau, P.; Michel, A. Polym Eng Sci 1998, 38, 1882.
20. Boyaud, M. F.; Cassagnau, P.; Michel, A.; Bousmina, M. Polym Eng Sci 2001, 41, 684.
21. Pesneau, I.; Cassagnau, P.; Michel, A. J Appl Polym Sci 2001, 82, 3568.
22. Cassagnau, P.; Michel, A. Polymer 2001, 42, 3139.
23. Semba, T.; Kitagawa, K.; Hamada, H.; Kwazuma, M.; Maeda, K. In: Proceedings of the 11th Annual Meeting of the Japan Society of Polymer Processing, 2000; p. 295.
24. Seibunkaisei Plastic Hand Book; NTS: Tokyo, Japan, 1995; p. 631.
25. Taylor, G. I. Proc R Soc London Ser A 0000, 146, 501.
26. Jansen, J. M. H.; Meijer, H. E. H. J Rheol 1993, 37, 597.
27. Huneault, M. A.; Shi, Z. H.; Utracki, L. A. Polym Eng Sci 1995, 35, 115.
28. Rumscheidt, F. D.; Mason, S. G. J Colloid Sci 0000, 16, 238.
29. Koubunshi Bunseki Hand Book; The Japan Society for Analytical Chemistry, Research Committee of Polymer Analysis: Japan, 1995.
30. Liedauer, S.; Eder, G.; Janeschitz-Kriegl, H.; Jerschow, P.; Geymayer, W. Ingolic, E. Int Polym Proc 1993, 8, 236.
31. Kumaraswamy, G.; Issaian, A. M.; Kornfield, J. A. Macromolecules 1999, 32, 7537.